

## Evaluation of adsorption properties of a porous carbon material from coffee waste

© Anastasia E. Memetova<sup>a</sup>✉, Nariman R. Memetov<sup>a</sup>, Andrey D. Zelenin<sup>a</sup>

<sup>a</sup> Tambov State Technical University, Bld. 2, 106/5, Sovetskaya St., Tambov, 392000, Russian Federation

✉ anastasia.90k@mail.ru

**Abstract:** The article investigates and evaluates the adsorption properties of a new highly porous carbon material in a wide range of pressures at temperatures above the critical level. It has been shown that the activated carbon material obtained from coffee waste is an effective adsorbent for CH<sub>4</sub>. So, in this study, carbonized coffee grounds were used as a precursor to obtain a highly porous carbon material (HPCM5), by chemical activation at 750 °C for efficient CH<sub>4</sub> adsorption. Porometry shows that the obtained adsorbent is micromesoporous with a narrow pore size distribution, having a BET specific surface area of 3456 m<sup>2</sup>·g<sup>-1</sup> and a pore volume of 1.604 cm<sup>3</sup>·g<sup>-1</sup>. The adsorption of CH<sub>4</sub> on the resulting carbon material was studied at temperatures of 298.15–323.15 K and pressures up to 100 bar. HPCM5 demonstrates a high CH<sub>4</sub> adsorption capacity of 19 mmol·g<sup>-1</sup> at 10 MPa and 298.15 K. Experimental data on CH<sub>4</sub> adsorption on HPCM5 were analyzed using typical Langmuir and Freundlich adsorption models in the temperature range 298.15–323.13 K. The results show that CH<sub>4</sub> adsorption on HPCM5 in the range of temperatures and pressures considered in this study correspond to the Langmuir adsorption; this is confirmed by the obtained values of the correlation coefficients equal to 0.99 and the average relative deviations between the experimental results and the results obtained with the Langmuir model, which are less than 3 %. The values of isosteric heats were calculated for different absolute amounts of CH<sub>4</sub> adsorption on the resulting HPCM5, which are in the range from ~10.0 to 17.0 kJ·mol<sup>-1</sup>. This characterizes the process as a physical adsorption, and the bond strength between the CH<sub>4</sub> molecule and adsorbent surface refers to the van der Waals force. The adsorption isotherm data and thermodynamic parameters evaluated in this study are useful for designing adsorption-based gas storage systems.

**Keywords:** adsorption; carbon adsorbent; methane; adsorption isotherms; adsorption isosteres; adsorption heat; porous structure.

**For citation:** Memetova AE, Memetov NR, Zelenin AD. Evaluation of adsorption properties of a porous carbon material from coffee waste. *Journal of Advanced Materials and Technologies*. 2023;8(3):207-216. DOI: 10.17277/jamt.2023.03.pp.207-216

## Оценка адсорбционных свойств пористого углеродного материала из «отработанного» кофе

© А. Е. Меметова<sup>a</sup>✉, Н. Р. Меметов<sup>a</sup>, А. Д. Зеленин<sup>a</sup>

<sup>a</sup> Тамбовский государственный технический университет,  
ул. Советская, 106/5, пом. 2, Тамбов, 392000, Российская Федерация

✉ anastasia.90k@mail.ru

**Аннотация:** Статья посвящена изучению и оценке адсорбционных свойств нового высокопористого углеродного материала в широком интервале давлений при температурах выше критической. Показано, что активированный углеродный материал, полученный из «отработанного кофе» является эффективным адсорбентом для CH<sub>4</sub>. Так, в данном исследовании карбонизированная кофейная гуща использовалась в качестве прекурсора для получения высокопористого углеродного материала (ВУМ5), путем химической активации при 750 °C для эффективной адсорбции CH<sub>4</sub>. Порометрия показывает, что полученный адсорбент является микромезопористым с узким

распределением пор по размерам, обладающий удельной площадью поверхности по БЭТ 3456 м<sup>2</sup>/г и объемом пор 1,604 см<sup>3</sup>/г. Изучена адсорбция CH<sub>4</sub> на полученном углеродном материале при температурах 298,15...323,15 К и давлении до 100 бар. ВУМ5 демонстрирует высокую адсорбционную способность по CH<sub>4</sub> 19 ммоль/г при 10 МПа и 298,15 К. Экспериментальные данные адсорбции CH<sub>4</sub> на ВУМ5 проанализированы с использованием типовых моделей адсорбции Ленгмюра и Фрейндлиха в интервале температур 298,15...323,13 К. Результаты показывают, что адсорбция CH<sub>4</sub> на ВУМ5 в рассматриваемом диапазоне температур и давлений соответствует адсорбции Ленгмюра. Данный факт подтверждается полученными значениями коэффициентов корреляции равными 0,99 и средних относительных отклонений между экспериментальными результатами и результатами, полученными с помощью модели Ленгмюра, которые составляют менее 3 %. Рассчитаны значения изостерических теплот при различных абсолютных количествах адсорбции CH<sub>4</sub> на полученном ВУМ5, которые находятся в диапазоне от ~10,0 до 17,0 кДж/моль, что указывает на то, что процесс представляет собой физическую адсорбцию, а сила связи между молекулой CH<sub>4</sub> и поверхностью адсорбента относится к силе Ван-дер-Ваальса. Данные изотерм адсорбции и термодинамические параметры, оцененные в настоящем исследовании, полезны для проектирования систем хранения газа на основе адсорбции.

**Ключевые слова:** адсорбция; углеродный адсорбент; метан; изотермы адсорбции; изостеры адсорбции; теплота адсорбции; пористая структура.

**Для цитирования:** Memetova AE, Memetov NR, Zelenin AD. Evaluation of adsorption properties of a porous carbon material from coffee waste. *Journal of Advanced Materials and Technologies*. 2023;8(3):207-216. DOI: 10.17277/jamt.2023.03.pp.207-216

## 1. Introduction

The greenhouse effect that causes global warming is the result of industrialization and the generation of gases such as methane (CH<sub>4</sub>), carbon dioxide (CO<sub>2</sub>), nitrogen oxide (N<sub>2</sub>O) and others. Although the concentration of CH<sub>4</sub> in the atmosphere is lower than that of CO<sub>2</sub>, the heating effect of CH<sub>4</sub> on a per molecule basis is 72 times greater than that of CO<sub>2</sub> [1]. Thus, the potential contribution of CH<sub>4</sub> emissions to global warming is 25 times higher than CO<sub>2</sub> [1]. At the concentration of CH<sub>4</sub> in the air of about 5–15 %, it is extremely explosive. When the concentration of CH<sub>4</sub> in the air reaches 30 %, it can cause headache, dizziness, fatigue, difficulty in breathing and rapid heartbeat, and even death by suffocation [2].

Adsorption is considered the most common approach to CH<sub>4</sub> removal because this method has several advantages including ease and simplicity of operation. Among various adsorbents, porous carbon materials are widely used for CH<sub>4</sub> removal due to their high specific surface area and total pore volume as well as a large number of surface functional groups [3].

In addition, the low sulphur and nitrogen content makes CH<sub>4</sub> a much cleaner burning fuel than commercial petrol [4]. Unfortunately, CH<sub>4</sub> has a low volumetric energy density, so its use is limited due to storage and transport problems. For this reason, its compression and storage is of great interest to the industrial and scientific community [5]. Current methods of CH<sub>4</sub> storage include its compression in

high-pressure tanks (compressed natural gas – CNG) and/or storage in liquefied form (liquefied natural gas – LNG). CNG is produced at pressures of more than 200 bar, which imposes certain requirements on the design of storage tanks (in particular, wall thickness), which are then quite difficult to place inside passenger cars [6]. Compression to these pressures is also costly [7]. LNG is stored at temperatures below 111 K (mainly used for intercontinental transport). The need for lower temperatures also incurs costs, requires well-insulated expensive tanks, and presents significant safety issues due to pressure build-up from CH<sub>4</sub> boil-off if the vehicles are left idle for long periods of time [8]. These problems have prompted the investigation of various alternatives to increase CH<sub>4</sub> density. An alternative to CNG and LNG is the use of adsorbents to store CH<sub>4</sub> (adsorbed natural gas – ANG) with higher density at ambient temperature and moderate pressure [9]. In fact, CH<sub>4</sub> storage in solid materials offers advantages in terms of gravimetric and volumetric energy density, safety and energy efficiency [10]. For this reason, ANG technology is considered a promising solution for energy storage, especially in natural gas-fueled vehicles [11].

The U.S. Department of Energy (DOE) has set requirements for the gravimetric and/or volumetric adsorption capacity of adsorbents for methane uptake (0.5 g CH<sub>4</sub>·g<sup>-1</sup> adsorbent and/or 263 cm<sup>3</sup> CH<sub>4</sub>·cm<sup>-3</sup> adsorbent) [12, 13]. Various nanoporous materials have been studied for CH<sub>4</sub> storage, including metal-organic frameworks (MOFs) [14, 15], nanoporous carbon [16, 17], porous polymers [18], etc.

Biochar, carbon-rich materials obtained by thermal decomposition of agricultural and industrial biomass wastes under oxygen-free conditions, has been widely recognised as a viable alternative to activated carbon for CH<sub>4</sub> adsorption due to several advantages including cost effectiveness and easy access to raw materials. Currently, coffee waste has emerged as an attractive candidate for biochar production [19]. According to the literature [20–23] because of its physicochemical properties, coffee waste can be used as a raw material (precursor) to produce porous carbon adsorbent and investigate it as a CH<sub>4</sub> adsorbent.

In this regard, the aim of the work is to evaluate the adsorption properties of a porous carbon material from used coffee grounds and assess its potential as effective materials for ANG technology.

## 2. Materials and Methods

### 2.1. Activation technique

The synthesis of a highly porous carbon material (HPCM5) was carried out by alkaline activation of carbonised used coffee grounds with potassium hydroxide. The mass ratio of "spent" coffee carbonisate: KOH during activation was 1 : 5. Activation was carried out in a pilot reactor in argon flow at 750 °C for 1 hour. After activation, excess KOH was removed with 0.1 M hydrochloric acid solution and then the product was washed with distilled water until a neutral pH value was reached.

### 2.2. Determination of specific surface area and adsorption characteristics

The porous structure of the adsorbent HPCM5 was characterised by N<sub>2</sub> adsorption-desorption isotherms at liquid nitrogen temperature (77 K) using an automatic surface and porosity analyser Autosorb-iQ (Quantachrome, USA).

The adsorption characteristics of HPCM5 were evaluated in the temperature range of 298.15–323.13 K and up to a final pressure of 10 MPa. The material was degassed at 350 °C for 2 h before the adsorption experiment. Measurements of CH<sub>4</sub> sorption under high pressure were performed with an iSorbHP high pressure and temperature gas adsorption analyser manufactured by Anton Paar GmbH using high purity CH<sub>4</sub> (99.999 %).

### 2.3. Theoretical basis

Adsorption isotherms demonstrate the correlation of adsorption amount with pressure under isothermal conditions and are often treated using

various sorption models [24]. The Langmuir (1) and Freundlich (2) models are the most widely used models.

Equation (1) is commonly used to describe adsorption data. This equation is based on gas adsorption by solids and is also known as monolayer adsorption theory [25]. With this model, it is assumed that adsorption occurs on a homogeneous solid surface.

$$a_L = \frac{Abp}{1 + bp}, \quad (1)$$

where  $a_L$  is the theoretical value of equilibrium gas adsorption according to the Langmuir model (mmol·g<sup>-1</sup>);  $p$  is the equilibrium pressure of the gas phase (MPa),  $A$  is the maximum adsorption capacity (mmol·g<sup>-1</sup>),  $b$  is the Langmuir adsorption constant, which depends on the properties of adsorbent, adsorbate and temperature. The larger the value of  $b$ , the higher the adsorption capacity of the material.

Equation (2) is an empirical formula that can be used to describe the theory of adsorption on a heterogeneous surface.

$$a_F = kp^{1/n}, \quad (2)$$

where  $a_F$  is the theoretical value of equilibrium gas adsorption according to the Freundlich model. In the formula,  $n$  and  $k$  are two empirical constants that depend on temperature. The value of  $k$  can be viewed as the amount of adsorption per unit of pressure. Generally speaking,  $k$  decreases with a temperature increase;  $n$  is the heterogeneity coefficient representing the adsorption capacity of the material and its value is usually greater than 1. When its value is greater than 1, it shows that the material has good adsorption capacity for CH<sub>4</sub>.

The validity of these models was assessed by the regression coefficient R<sup>2</sup>, which ranges from 0 to 1, and the normalized standard deviation  $\Delta a$  (%) defined as:

$$\Delta a = 100 \sqrt{\frac{\sum_{i=1}^n [(a_{\text{exp}} - a_{\text{mod}})/a_{\text{exp}}]^2}{N - 1}}, \quad (3)$$

where  $a_{\text{exp}}$  and  $a_{\text{mod}}$  are the gas adsorption values obtained from experiments and theoretical models, respectively,  $N$  is the number of data points of the adsorption isotherm.

The isosteric heat of adsorption is the enthalpy change that occurs during the adsorption process. It is calculated using the Clausius–Clapeyron equation [26]:

**Table 1.** Textural properties of the HPCM5 nanoporous carbon material

$S_{\text{BET}}$	$S_{\text{DFT}}$	$V_{\text{DFT}}$	$V_0 = V_{01} + V_{02}$	$V_{03}$	$V_{01}$	$V_{02}$	$D_{01}$	$D_{02}$	$D_{03}$
$\text{m}^2 \cdot \text{g}^{-1}$		$\text{cm}^3 \cdot \text{g}^{-1}$			nm				
3456	2469	1.604	0.739	0.865	0.401	0.338	0.92	1.61	3.09

where  $S_{\text{BET}}$  is the specific surface area by nitrogen calculated using the Brunauer–Emmett–Teller method;  $S_{\text{DFT}}$  is the specific surface area by nitrogen calculated using density functional theory;  $V_{01}$  is the specific pore volume of the first mode;  $V_{02}$  is the specific volume of pores of the second mode;  $V_0$  is the specific volume of micropores;  $V_{03}$  is the specific volume of pores of mesopores;  $D_{01}$  is the average diameter (width) of pores of the first mode;  $D_{02}$  is the average diameter (width) of pores of the second mode;  $D_{03}$  is the average diameter (width) of pores of the third mode.

$$\left(\frac{d \ln p}{dT}\right)_n = -\frac{q_{st}}{RT^2}, \quad (4)$$

where  $R$  is the ideal gas constant,  $8.314 \text{ J} \cdot (\text{mol} \cdot \text{K})^{-1}$ ,  $T$  is the temperature (K),  $n$  is the specific amount adsorbed at pressure  $p$  and temperature  $T$ .

Hence:

$$q_{st} = -R \left(\frac{d \ln p}{d(1/T)}\right)_n. \quad (5)$$

### 3. Results and Discussion

#### 3.1. Surface and porosity characteristics of HPCM

An important characteristic of each adsorbent is its specific surface area, which strongly influences its adsorption capacity. The values of specific surface area, micropore volume (less than 2 nm) and mesopore volume (2–50 nm) are good indicators of successful synthesis of HPCM prior to adsorption studies.

The pore parameters of the synthesised highly porous carbon material are summarised in Table 1.

The HPCM5 sample used in this study is a micromesoporous material ( $V_0 = 0.739 \text{ cm}^3 \cdot \text{g}^{-1}$ ;  $V_{03} = 0.865 \text{ cm}^3 \cdot \text{g}^{-1}$ ) with a narrow pore size distribution (less than 5 nm). The analysis showed that HPCM5 possesses a multimodal pore size distribution calculated using density functional theory (DFT); in particular, there are micropore peaks with maxima around 0.9 and 1.6 nm, as well as a mesopore peak with a maximum around 3.1 nm (Table 1). In addition, it should be noted that HPCM5 possesses a BET specific surface area of  $3456 \text{ m}^2 \cdot \text{g}^{-1}$  and a pore volume of  $1.604 \text{ cm}^3 \cdot \text{g}^{-1}$ .

#### 3.2. Adsorption characteristics of HPCM

Experimental data at six different temperatures (from 298.15 to 323.15K) were processed using the Langmuir and Freundlich models. Figure 1 shows the dependence of  $\text{CH}_4$  sorption on the investigated HPCM5 sample in coordinates of the Langmuir and Freundlich models.

The  $\text{CH}_4$  adsorption isotherms measured at temperatures 298.15, 303.15, 308.15, 313.15, 318.15, 323.15 K and pressure up to 10 MPa on the HPCM5 sample and the results of modelling of isothermal adsorption curves are presented in Fig. 2. The lines correspond to the Langmuir and Freundlich models and the dots represent the experimental data. The estimated Langmuir and Freundlich parameters for  $\text{CH}_4$  on the HPCM5 sample at six different temperatures are given in Tables 2 and 3.

As can be seen from Fig. 2, the equilibrium adsorbed amounts of  $\text{CH}_4$  increase with increasing pressure in the system, but the slope of the curves decreases at higher pressures, since in this case the adsorption centers approach saturation. In addition, Fig. 2 shows that temperature strongly affects the equilibrium adsorption capacity all else being equal. That is, as the adsorption temperature increases, the amount of adsorbed  $\text{CH}_4$  decreases, which is due to the heat release during  $\text{CH}_4$  adsorption. The maximum value of adsorption capacity of HPCM5 on  $\text{CH}_4$  is  $19 \text{ mmol} \cdot \text{g}^{-1}$  at 10 MPa and 298.15 K.

Figure 2a shows that the experimental data are in excellent agreement with the Langmuir model, which indicates that this isothermal model can be used to describe the investigated adsorption equilibrium. Another confirmation of the applicability of the Langmuir model to describe the obtained experimental data is the high value of the correlation coefficient  $R^2$  (more than 0.99) and the

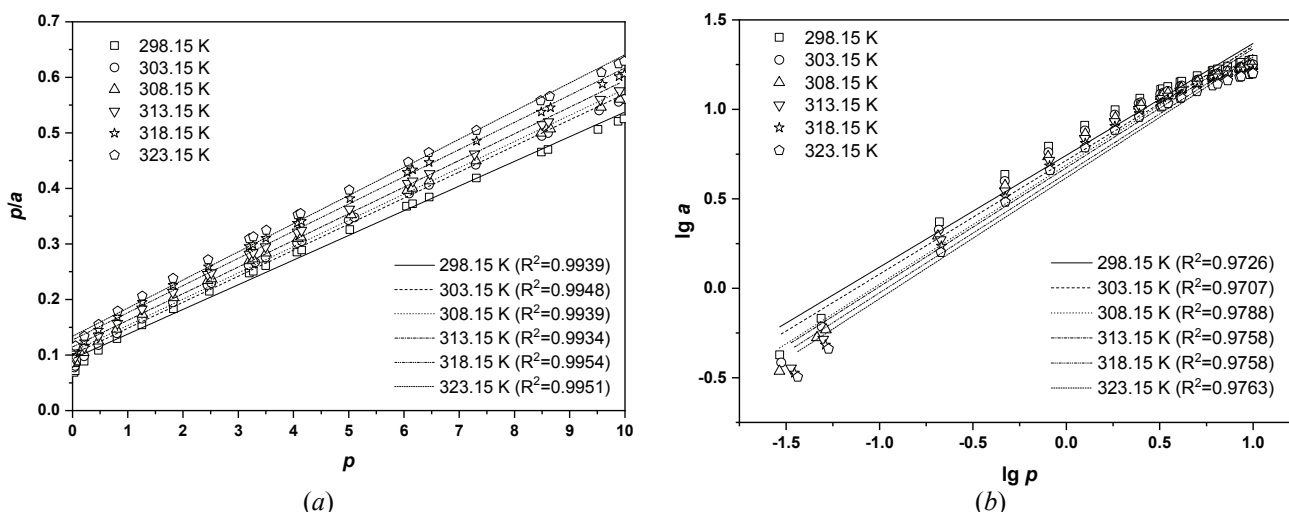


Fig. 1. Dependence of CH<sub>4</sub> sorption on HPCM5 in the coordinates of the Langmuir (a) and Freundlich (b) models

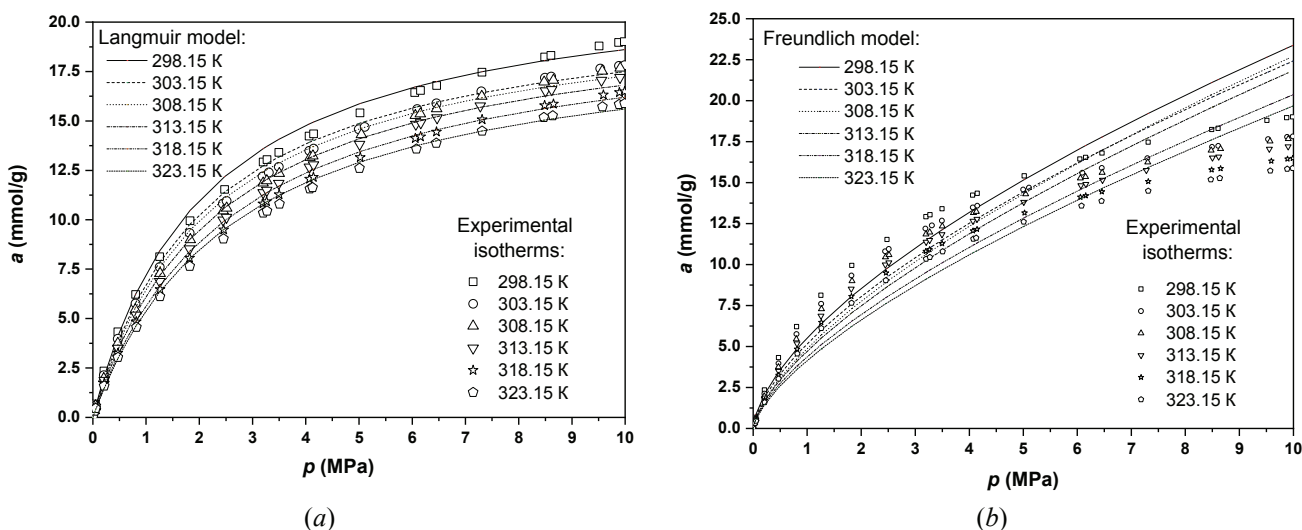


Fig. 2. CH<sub>4</sub> adsorption isotherms on HPCM5 at different temperatures, adapted according to the Langmuir (a) and Freundlich (b) models

Table 2. Adsorption isotherm coefficients for the Langmuir model

Temperature, K	$a_{exp}$	Langmuir constants				
		$a_L$ mmol·g <sup>-1</sup>	$A$	$b$	$R^2$	$\Delta a, \%$
298.15	19.01	18.61	22.52	0.476	0.9939	8.97
303.15	17.81	17.49	21.23	0.468	0.9948	7.75
308.15	17.67	17.23	21.14	0.445	0.9939	8.14
313.15	17.20	16.79	20.83	0.419	0.9934	6.69
318.15	16.48	16.19	20.41	0.385	0.9954	6.56
323.15	15.88	15.60	19.72	0.379	0.9951	5.77

**Table 3.** Adsorption isotherm coefficients for the Freundlich model

Temperature, K	Freundlich constants					$\Delta a, \%$
	$a_{\text{exp}}$ mmol·g <sup>-1</sup>	$a_F$	$k$	$n$	$R^2$	
298.15	19.01	23.35	5.54	1.59	0.9726	17.89
303.15	17.81	22.41	5.19	1.57	0.9707	18.51
308.15	17.67	22.57	4.89	1.50	0.9788	17.61
313.15	17.20	21.70	4.73	1.50	0.9758	17.34
318.15	16.48	20.35	4.38	1.49	0.9758	17.97
323.15	15.88	19.66	4.14	1.48	0.9763	17.82

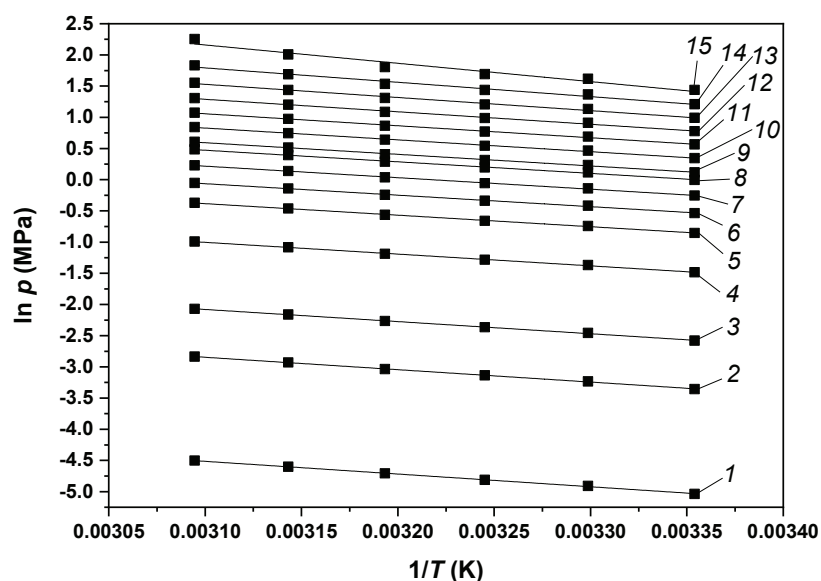
low value of the normalised standard deviation  $\Delta a$  (less than 10 %) (Table 2). Also, it should be noted that the values of theoretical values  $a_L$  of CH<sub>4</sub> adsorption on the HPCM5 sample obtained by the Langmuir model at different temperatures have a deviation from the experimentally obtained adsorption values  $a_{\text{exp}}$  of less than 3 %. However, as can be seen from Fig. 2b, the Freundlich model showed the worst agreement with the obtained experimental data of CH<sub>4</sub> adsorption on HPCM5 ( $R^2 \approx 0.97$ ;  $\Delta a \approx 18\%$ ) (see Table 3).

Table 2 shows that the maximum adsorption value and Langmuir parameters decrease with increasing temperature. The increase in temperature leads to CH<sub>4</sub> molecules becoming more active and more difficult to retain on the surface of the HPCM5, which reduces the adsorption capacity. The value of the Langmuir parameter  $b$  shows the affinity of CH<sub>4</sub>

molecules to the adsorbent surface, and when it decreases (Table 2), it indicates a gradual decrease in the affinity of CH<sub>4</sub> molecules to the HPCM5 surface with a temperature rise.

Experimental CH<sub>4</sub> adsorption isotherms were used to plot the isosteres, which represent the quantitative relationship between pressure and temperature at a constant adsorption value (Fig. 3).

Generally, the value of isosteric heat of adsorption ( $q_{st}$ ) depends on the absolute value of adsorption [27]. Hence, the  $q_{st}$  values for the investigated sample were calculated for fifteen different absolute adsorption quantities equal to 0.1, 0.5, 1.0, 2.5, 4.0, 5.0, 6.0, 7.0, 7.5, 8.5, 9.5, 9.5, 10.5, 11.5, 12.5 and 13.5 mmol·g<sup>-1</sup>. As can be seen from Fig. 3, the isosteres of CH<sub>4</sub> adsorption on HPCM5, plotted as the dependence of  $\ln(p)$  on  $(1/T)$ , are well approximated by a straight line.



**Fig. 3.** The isosteres of CH<sub>4</sub> adsorption on HPCM5 during the adsorption process, mmol·g<sup>-1</sup>: 0.1 (1), 0.5 (2), 1.0 (3), 2.5 (4), 4.0 (5), 5.0 (6), 6.0 (7), 7.0 (8), 7.5 (9), 8.5 (10), 9.5 (11), 10.5 (12), 11.5 (13), 12.5 (14), and 13.5 (15)

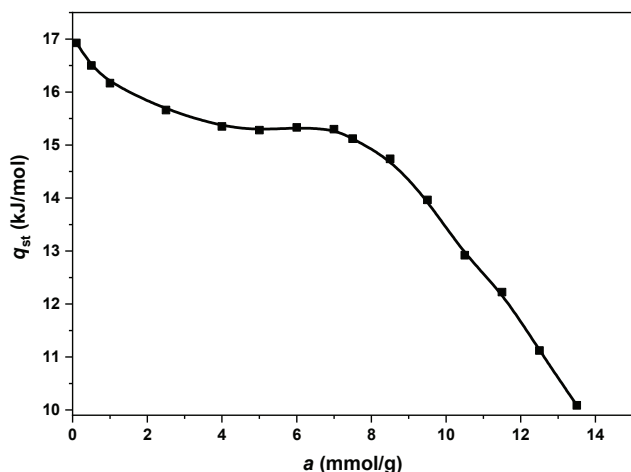


Fig. 4. Isosteric heat of adsorption of CH<sub>4</sub> on HPCM5

The dependence of isosteric heat on the value of CH<sub>4</sub> adsorption on HPCM5 is shown in Fig. 4. As can be seen in the figure,  $q_{st}$  calculated by the Clausius–Clapeyron equation decreases with increasing adsorption amount. Also for the studied adsorption system, a high value of  $q_{st}$  is observed at the early stages of adsorption, when CH<sub>4</sub> molecules occupy most of the micropores, binding to high-energy adsorption centres.

Thus, at low adsorbate loadings, the absolute value of  $q_{st}$  depends on the density of adsorption centres, which are high-energy micropores with sizes comparable to those of adsorbate molecules. As the number of adsorbed molecules increases, the high-energy adsorption centres are completely filled and the adsorbate-adsorbate interactions contribute to the heat of adsorption. Thus, the dependence  $q_{st} = f(a)$  reflects the change in the state of adsorbed molecules during adsorption – from binding to high-energy adsorption centres to the formation of molecular associates and their subsequent rearrangement close to saturation.

The  $q_{st}$  values at different absolute adsorption quantities for the HPCM5 sample range from ~17.0 to 10.0 kJ·mol<sup>-1</sup>.

Since the heat of chemical adsorption usually ranges from 40 to 600 kJ·mol<sup>-1</sup>, this indicates that the predominant adsorption process of CH<sub>4</sub> on the investigated sample is physical adsorption [28], and the bonding force between the CH<sub>4</sub> molecule and the adsorbent surface refers to the van der Waals force [29].

From the practical side of the issue of calculating the ANG system capacity, the absolute content adsorption value is not indicative, since it takes into account only CH<sub>4</sub> in the adsorbed state. However, in order to understand the total capacity,

the gas phase in the space between the granules of porous materials should also be considered. The volumetric active specific capacity of the system and the adsorption active gravimetric capacity of the porous materials are important for the performance of the ANG system.

The CH<sub>4</sub> adsorption capacity of the HPCM5 has been measured at 298 K and pressures up to 10 MPa. Levels of gravimetric and volumetric adsorption of methane on HPCM5 are shown in Fig. 5.

Thus, HPCM5 showed a gravimetric adsorption of 0.51 g·g<sup>-1</sup> (106 m<sup>3</sup> (STP) · m<sup>-3</sup>) at the corresponding pressure of 10 MPa and temperature of 298 K. However, due to the low packing density, the obtained experimental data on CH<sub>4</sub> volumetric adsorption are somewhat lower than required for the application of the considered materials as adsorbents for ANG technology.

It is possible to solve this problem, namely to increase the volumetric capacity of carbon structures for CH<sub>4</sub> storage, by increasing the packing density, i.e. by reducing the space between the granules. However, in this case it is also necessary to optimize the packing parameters, investigating the influence of key conditions of the process implementation (compaction pressure, type of binder, degree of adsorbent dispersion, as well as the size and shape of adsorbent particles) on the properties of the obtained materials. Also, it is necessary to control the nature of pore structure change during mechanical compaction.

In order to evaluate the potential of HPCM5 as adsorbents for ANG technology, it is important to compare the gravimetric CH<sub>4</sub> adsorption capacity with other commonly investigated adsorbents. Figure 6 presents a comparison of the gravimetric CH<sub>4</sub> uptake

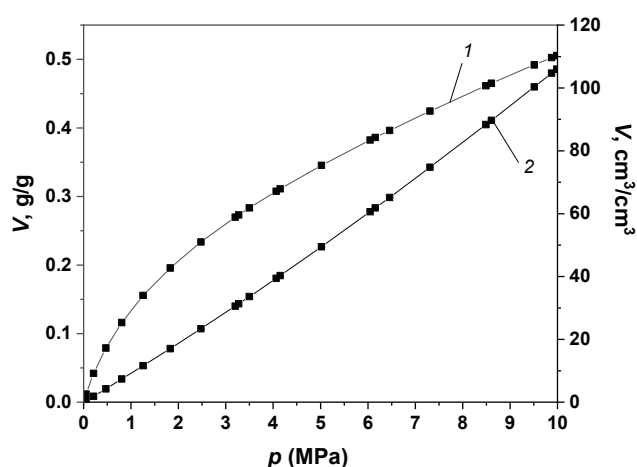
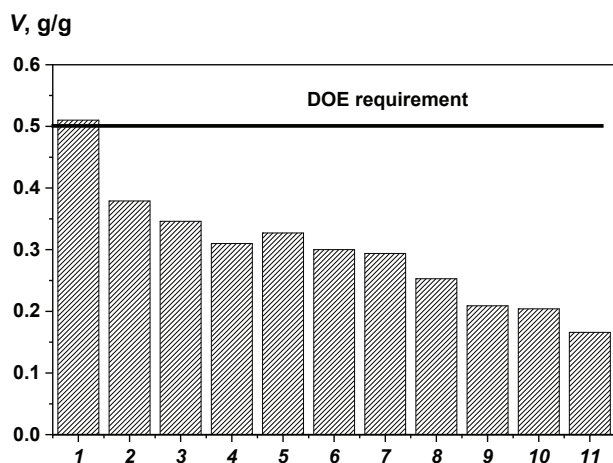


Fig. 5. Plotting of gravimetric (1) and volumetric (2) absorptions of methane  $V$  from pressure  $p$  up to 10 MPa on HPCM5 adsorbent at 298 K



**Fig. 6.** Comparison of CH<sub>4</sub> operating capacities for selected methane adsorbents:

1 – this study; 2 – BUT-22; 3 – PPN-4; 4 – AX-21; 5 – ZJU-36; 6 – Maxsorb III; 7 – MOF-5; 8 – NOTT-102; 9 – UTSA-76; 10 – Co(bdp); 11 – HKUST-1

for some selected methane adsorbents: BUT-22 (296 K, 8 MPa), PPN-4 (298 K, 5.5 MPa), AX-21 (248 K, 10 MPa), ZJU-36 (240 K, 6.5 MPa), Maxsorb III (298 K, 8 MPa), MOF-5 (248 K, 10 MPa) NOTT-102 (273 K, 6.5 MPa) UTSA-76 (273 K, 6.5 MPa) Co(bdp) (273 K, 6.5 MPa), HKUST-1 (298 K, 10 MPa) [30–41].

The results show that the gravimetric capacity of HPCM5 exceeds the gravimetric working capacity of the examined CH<sub>4</sub> adsorbents. Since such properties as surface area, pore volume and packing density of carbon materials can be adjusted during synthesis, the materials obtained from coffee waste have a high potential for their use as adsorbents for ANG technology. In addition, adsorbents derived from coffee waste can be cheaper to produce than metal-organic frameworks (MOFs), which currently show high adsorption capacities towards CH<sub>4</sub>.

#### 4. Conclusion

Activated carbon material obtained from coffee waste is an effective CH<sub>4</sub> adsorbent. The sample of highly porous carbon material (HPCM5) used in this study is a micromesoporous adsorbent having a BET specific surface area of 3456 m<sup>2</sup>·g<sup>-1</sup> and a pore volume of 1.604 cm<sup>3</sup>·g<sup>-1</sup>.

The adsorption of CH<sub>4</sub> on HPCM5 has been investigated and the experimental data have been analysed using the Langmuir and Freundlich adsorption models in the temperature range 298.15–323.13 K and pressure up to 10 MPa. The results show that the adsorption of CH<sub>4</sub> on HPCM5 over the range of temperatures and pressures considered in

this study is consistent with the Langmuir adsorption, and this is confirmed by the high values of the correlation coefficient (greater than 0.99) and low values of the normalised standard deviation (less than 10 %). In addition, it is found that the average relative deviations between the experimental results and the data obtained using the Langmuir model are less than 3 %. The maximum value of CH<sub>4</sub> adsorption capacity of HPCM5 is 19 mmol·g<sup>-1</sup> at 298.15 K and 10 MPa.

Adsorption isosteres are plotted. The dependence of isosteric heat of adsorption of CH<sub>4</sub> on HPCM5 was calculated. It is shown that the values of isosteric heat at different absolute amounts of adsorption for the sample of HPCM5 decrease from ~17.0 to 10.0 kJ·mol<sup>-1</sup>.

The adsorption capacity of HPCM5 was studied in terms of gravimetric and volumetric capacity for CH<sub>4</sub> at 293 K and pressure up to 10 MPa. It was found that the level of gravimetric adsorption of CH<sub>4</sub> corresponds to the requirements formed by the U.S. Department of Energy, and the HPCM5's volumetric specific capacity for CH<sub>4</sub> is slightly lower than DOE requirements, due to low packing density.

It is worth noting that the performance characteristics of carbon materials derived from used coffee grounds are generally comparable to adsorbents of other classes. However, the experimental data indicate that the resultant materials have a high potential and that further studies are needed to optimise the physicochemical and functional properties of the adsorbents.

#### 5. Funding

The work has been carried out with the financial support of the President of the Russian Federation Scholarship Programme (SP-1260.2021.1).

#### 6. Conflict of interests

The authors declare no conflict of interests.

#### References

1. Refaat TF, Ismail S, Nehrir AR, Hair JW, Crawford JH, Leifer I, Shuman T. Performance evaluation of a 1.6- $\mu\text{m}$  methane DIAL system from ground, aircraft and UAV platforms. *Optics Express*. 2013;21:30415-30432. DOI:10.1364/OE.21.030415
2. Massie C, Stewart G, McGregor G, Gilchrist JR. Design of a portable optical sensor for methane gas detection. *Sensors and Actuators B: Chemical*. 2006;113:830-836. DOI:10.1016/j.snb.2005.03.105
3. Morris JR, Contescu CI, Chisholm MF, Cooper VR, Guo J, He L, et al. Modern approaches to studying gas

- adsorption in nanoporous carbons. *Journal of Materials Chemistry A*. 2013;1:9341-9350. DOI:10.1039/C3TA10701A
4. Alcañiz-Monge D, Lozano-Castelló D, Cazorla-Amorós A, Linares-solano fundamentals of methane adsorption in microporous carbons. *Microporous and Mesoporous Materials*. 2009;124(1-3):110-116. DOI: 10.1016/j.micromeso.2009.04.041
  5. Casco ME, Martínez-Escandell M, Gadea-Ramos E, Kaneko K, Silvestre-Albero J, Rodríguez-Reinoso F. High-pressure methane storage in porous materials: are carbon materials in the pole position? *Chemistry of Materials*. 2015;27:959-964. DOI:10.1021/cm5042524
  6. Policicchio A, Filosa R, Abate S, Desiderio G, Colavita E. Activated carbon and metal organic framework as adsorbent for low-pressure methane storage applications: an overview. *Journal of Porous Materials*. 2017;24:905-922. DOI:10.1007/s10934-016-0330-9
  7. Wang XL, French J, Kandadai S, Chua HT. Adsorption measurements of methane on activated carbon in the temperature range (281 to 343) K and pressures to 1.2 MPa. *Journal of Chemical & Engineering Data*. 2010;55:2700-2706. DOI:10.1021/jc900959w
  8. Kumar KV, Kathrin O, Titirici M-M, Rodríguez-Reinoso M-M. Nanoporous materials for the onboard storage of natural gas. *Chemical Reviews*. 2017;117:1796-1825. DOI:10.1021/acs.chemrev.6b00505
  9. Bimbo N, Smith JP, Aggarwal H, Physick AJ, Pugsley A, Barbour LJ, Ting VP, Mays TJ. Kinetics and enthalpies of methane adsorption in microporous materials AX-21, MIL-101 (Cr) and TE7. *Chemical Engineering Research and Design*. 2021;169:153-164. DOI:10.1016/j.cherd.2021.03.003
  10. Mason JA, Veenstra M, Long JR. Evaluating metal-organic frameworks for natural gas storage. *Chemical Science*. 2014;5:32-51. DOI:10.1039/C3SC52633J
  11. Nour UM, Tayeb AM, Farag HA, Awad S. Enhanced discharge of ANG storage for vehicle use. *International Journal of Engineering & Technology*. 2009;9:381-389.
  12. Beckner M, Dailly A. Adsorbed methane storage for vehicular applications. *Applied Energy*. 2015;149:69-74. DOI:10.1016/j.apenergy.2015.03.123
  13. DoE technical targets for hydrogen storage systems for material handling equipment fuel cell technologies office. *Office of energy efficiency & renewable energy, energy.gov*. Available from: <https://www.energy.gov/eere/fuelcells/doe-technical-targets-hydrogen-storage-systems-material-handling-equipment> [Accessed 21 July 2023].
  14. The advanced research projects agency – Energy (ARPA-E) of the U.S department of energy. *DE-FOA-0000672: Methane Opportunities for Vehicular Energy (MOVE)*. Available from: <https://arpa-e-foa.energy.gov/Default.aspx?Search=move&SearchType=https://arpa-e-foa.energy.gov/Default.aspx?Search=move&SearchType=#FoaIddc1d731e-f2cf-4be9-b6ac-ab315582d000> [Accessed 21 July 2023].
  15. Konstas K, Osl T, Yang Y, Batten M, Burke N, Hill AJ, Hilla MR. Methane storage in metal organic frameworks. *Journal of Materials Chemistry*. 2012;22:16698-16708. DOI:10.1039/C2JM32719H
  16. Sharafinia S, Rashidi A, Babaei B. et al. Nanoporous carbons based on coordinate organic polymers as an efficient and eco-friendly nano-sorbent for adsorption of phenol from wastewater. *Scientific Reports*. 2023;13:13127. DOI:10.1038/s41598-023-40243-0
  17. Park J, Jung M, Jang L, Lee K, Attia NF, Oh H. A facile synthesis tool of nanoporous carbon for promising H<sub>2</sub>, CO<sub>2</sub>, and CH<sub>4</sub> sorption capacity and selective gas separation. *Journal of Materials Chemistry*. 2018;6:23087-23100. DOI:10.1039/C8TA08603F
  18. Choi P-S, Jeong J-M, Choi Y-K, Kim M-S, Shin G-J, Park S-J. A review: methane capture by nanoporous carbon materials for automobiles. *Carbon Letters*. 2016;17:18-28. DOI:10.5714/CL.2016.17.1.018
  19. Tong W, Lv Y, Svec F. Advantage of nanoporous styrene-based monolithic structure over beads when applied for methane storage. *Applied Energy*. 2016;183:1520-1527. DOI:10.1016/j.apenergy.2016.09.066
  20. Alshareef SA, Alqadami AA, Khan MA, Alanazi HS, Siddiqui MR, Jeon B-H. Simultaneous co-hydrothermal carbonization and chemical activation of food wastes to develop hydrochar for aquatic environmental remediation. *Bioresource Technology*. 2021;126363. DOI:10.1016/j.biortech.2021.126363
  21. Tehrani NF, Aznar JS, Kiros Y. Coffee extract residue for production of ethanol and activated carbons. *Journal of Cleaner Production*. 2015;91:64-70. DOI:10.1016/j.jclepro.2014.12.031
  22. Wang H, Li X, Cui Z, Fu Z, Yang L, Liu G, Li M. Coffee grounds derived N enriched microporous activated carbons: efficient adsorbent for post-combustion CO<sub>2</sub> capture and conversion. *Journal of Colloid and Interface Science*. 2020;578:491-499. DOI: 10.1016/j.jcis.2020.05.125
  23. Paredes-Laverde M, Salamanca M, Diaz-Corrales JD, Flórez E, Silva-Agredo J, Torres-Palma RA. Understanding the removal of an anionic dye in textile wastewaters by adsorption on ZnCl<sub>2</sub> activated carbons from rice and coffee husk wastes: A combined experimental and theoretical study. *Journal of Environmental Chemical Engineering*. 2021;9:105685. DOI:10.1016/j.jece.2021.105685
  24. Thithai V, Jin X, Ajaz Ahmed M, Choi JW. Physicochemical properties of activated carbons produced from coffee waste and empty fruit bunch by chemical activation method. *Energies*. 2021;14:3002. DOI:10.3390/en14113002
  25. Tang X, Ripepi N, Luxbacher K, Pitcher E. Adsorption models for methane in shales: Review, Comparison, and application. *Energy & Fuels*. 2017;31(10):10787-10801. DOI:10.1021/acs.energyfuels.7b01948
  26. Du X, Cheng Y, Liu Z, Yin H, Wu T, Huo L, et al. CO<sub>2</sub> and CH<sub>4</sub> adsorption on different rank coals: a thermodynamics study of surface potential, Gibbs free energy change and entropy loss. *Fuel*. 2021;283:118886. DOI:10.1016/j.fuel.2020.118886
  27. Álvarez-Gutiérrez N, Gil MV, Rubiera F, Pevida C. Adsorption performance indicators for the CO<sub>2</sub>/CH<sub>4</sub> separation: application to biomass-based activated carbons.

- Fuel Processing Technology.* 2016;142:361-369. DOI:10.1016/j.fuproc.2015.10.038
28. Tian H, Li TF, Zhang TW, et al. Characterization of methane adsorption on overmature Lower Silurian-Upper Ordovician shales in Sichuan Basin, southwest China: experimental results and geological implications. *International Journal of Coal Geology.* 2016;156:36-49. DOI:10.1016/j.coal.2016.01.013
29. Yang F, Ning ZF, Wang Q, Liu HQ, Kong DT. Thermodynamic analysis of methane adsorption on gas shale. *Journal of Central South University, Science and Technology.* 2014;45:2871-2877.
30. Zhou SW, Wang HY, Zhang PY, et al. Investigation of the isosteric heat of adsorption for supercritical methane on shale under high pressure. *Adsorption Science & Technology.* 2019;37:590-606. DOI:10.1177/0263617419866986
31. Mason JA, Oktawiec J, Taylor MK. Methane storage in flexible metal-organic frameworks with intrinsic thermal management. *Nature.* 2015;527:357-361. DOI:10.1038/nature15732
32. Peng Y, Krungleviciute V, Eryazici I. Methane storage in metal-organic frameworks: current records, surprise findings, and challenges. *Journal of the American Chemical Society.* 2013;135:11887-11894. DOI:10.1021/ja4045289
33. Yuan D, Lu W, Zhao D, Zhou H-C. Highly stable porous polymer networks with exceptionally high gas-uptake capacities. *Advanced Materials.* 2011;23(32):3723-3725. DOI:10.1002/adma.201101759
34. Alezi D, Belmabkhout Y, Suyetin M. MOF crystal chemistry paving the way to gas storage needs: aluminum-based SOC-MOF for CH<sub>4</sub>, O<sub>2</sub>, and CO<sub>2</sub> storage. *Journal of the American Chemical Society.* 2015;137:13308-13318. DOI: 10.1021/jacs.5b07053
35. Kong G-Q, Han Z-D, He Y. Expanded organic building units for the construction of highly porous metal-organic frameworks. *Chemistry A European Journal.* 2013;19(44):14886-14894. DOI:10.1002/chem.201302515
36. He Y, Zhou W, Yildirim T, Chen B. A series of metal-organic frameworks with high methane uptake and an empirical equation for predicting methane storage capacity. *Energy & Environmental Science.* 2013;6:2735-2744. DOI:10.1039/c3ee41166d
37. Wang B, Zhang X, Huang H. A microporous aluminum-based metal-organic framework for high methane, hydrogen, and carbon dioxide storage. *Nano Research.* 2021;14:507-511. DOI:10.1007/s12274-020-2713-0
38. Al-Naddaf Q, Majedi Far H, Cheshomi N. Exceptionally high gravimetric methane storage in aerogel-derived carbons. *Industrial & Engineering Chemistry Research.* 2020;59:19383-19391. DOI: 10.1021/acs.iecr.0c03225
39. Li B, Wen H-M, Zhou W. Porous metal-organic frameworks: promising materials for methane storage. *Chem.* 2016;1(4):557-580. DOI:10.1016/j.chempr.2016.09.009
40. Thu K, Kim Y-D, Ismil AB. Adsorption characteristics of methane on Maxsorb III by gravimetric method. *Applied Thermal Engineering.* 2014;72(2):200-205. DOI:10.1016/j.applthermaleng.2014.04.076
41. Wegrzyn J, Wisemann H, Lee Wegrzyn T, Low J. Pressure storage of natural gas on activated carbon. *SAE Proceeding of Annual Automotive Technology.* 1992:1-11.
42. Rozyyev V, Thirion D, Ullah R. et al. High-capacity methane storage in flexible alkane-linked porous aromatic network polymers. *Nature Energy.* 2019;4:604-611. DOI:10.1038/s41560-019-0427-x

### Information about the authors / Информация об авторах

**Anastasia E. Memetova**, Cand. Sc. (Eng.), Associate Professor of the Department, Tambov State Technical University (TSTU), Tambov, Russian Federation; ORCID 0000-0002-1036-7389; e-mail: anastasia.90k@mail.ru

**Nariman R. Memetov**, Cand. Sc. (Eng.), Associate Professor, Head of the Department, TSTU, Tambov, Russian Federation; ORCID 0000-0002-7449-5208; e-mail: memetov.nr@mail.tstu.ru

**Andrey D. Zelenin**, Junior Researcher, TSTU, Tambov, Russian Federation; AuthorID (Scopus) 41763210800; e-mail: zeleandrey@yandex.ru

**Меметова Анастасия Евгеньевна**, кандидат технических наук, доцент кафедры, Тамбовский государственный технический университет (ТГТУ), Тамбов, Российская Федерация; ORCID 0000-0002-1036-7389; e-mail: anastasia.90k@mail.ru

**Меметов Нариман Рустемович**, кандидат технических наук, доцент, заведующий кафедрой, ТГТУ, Тамбов, Российская Федерация; ORCID 0000-0002-7449-5208; e-mail: memetov.nr@mail.tstu.ru

**Зеленин Андрей Дмитриевич**, младший научный сотрудник, ТГТУ, Тамбов, Российская Федерация; AuthorID (Scopus) 41763210800; e-mail: zeleandrey@yandex.ru

*Received 31 May 2023; Accepted 05 July 2023; Published 06 October 2023*



**Copyright:** © Memetova AE, Memetov NR, Zelenin AD, 2023. This article is an open access article distributed under the terms and conditions of the Creative Commons Attribution (CC BY) license (<https://creativecommons.org/licenses/by/4.0/>).